Proton-Proton Scattering at 240 Mev by a Magnetic Deflection Method*

O. A. Towler, Jr.†‡
University of Rochester, Rochester, New York
(Received November 14, 1951)

Differential cross sections for proton-proton scattering have been measured at eight angles ranging from 171.3° to 108.1° center of mass by magnetically deflecting protons scattered by hydrocarbon and carbon targets into photographic plates placed inside the tank of the Rochester 130″ cyclotron. The incident beam was monitored by the beta-activity induced in the target by the reaction $C^{12}(p,pn)C^{11}$, the absolute value of the cross section being based on a 49±3 mb carbon cross section. The measured cross section is isotropic within statistical errors from 108° to 167°, with an average value of 4.66±0.39 millibarns/steradian, and increases sharply to a value of 15.8±1.6 mb at 171.3°. The average value of the cross section agrees with that of Oxley and Schamberger, but is in disagreement with the value obtained by Chamberlain, Segrè, and Wiegand.

I. INTRODUCTION

DETERMINATIONS of proton-proton scattering cross sections at 240 Mev were undertaken by a method differing from the coincidence counter measurements of Oxley and Schamberger[1] of this laboratory in the method of counting the scattered protons. The reasons were to provide a check on the counter experiment and to extend the angular range of the measurements. The measurement of the differential scattering cross section has been extended to 8.7° c.m.[2]

The experimental method, which has been described briefly before,[3] was to use the magnetic field of the cyclotron to deflect protons scattered by a hydrocarbon target into photographic plates placed in the cyclotron tank. When properly shielded nuclear track sensitive photographic plates are inserted in the cyclotron tank near the lower pole tip of the magnet, a part of the protons scattered from the internal circulating beam by the protons in a hydrocarbon target describe helical paths and enter the plates at an angle directly related to the scattering angle. These protons enter in a well-collimated group, while those scattered by the carbon nuclei arrive uncollimated. The number of protons scattered by protons is obtained from the difference in the number entering a plate in a certain range of entrance angle when scattered by a hydrocarbon and a carbon target. The beam incident on the target is monitored by the radioactivity induced in the carbon of the target.

The laboratory cross section, $\sigma(\theta)$, is given by

$$\sigma(\theta)=\frac{N_P(\theta)\sigma_C \mathrm{C/H}}{N_C\Delta\Omega(\theta)}, \quad (1)$$

where $N_P(\theta)$ is the number of protons scattered by protons at an angle θ into the solid angle $\Delta\Omega(\theta)$, σ_C the production cross section for C^{11} at 240 Mev, C/H the ratio of carbon to hydrogen atoms in the target, and N_C the number of C^{11} atoms produced at the time of exposure of the plates.

The C:H ratio in the polyethylene $(CH_2)_n$ targets was determined by Wichers and Paulson of the National Bureau of Standards to be 1:2 within 0.2 percent. The production cross section of C^{11} was taken to be 49±3 mb[4] at 240 Mev. The incident proton energy, 240 Mev, was determined by range measurements in copper and by consideration of the geometry and expected entrance angle for proton-proton collisions in the apparatus to be described. The determination of the other factors in Eq. (1) will now be considered in some detail.

II. APPARATUS

A. General Description

A plan view of the apparatus showing the target at the 58.5-inch radius used, plate holder positions, and shielding is given in Fig. 1. The target holder probe was inserted in the median plane of the tank, while the plate holder probe was inserted 4.21″ below the median plane through one of two flanges, making different angles with the radius to the target. The flanges could be moved horizontally to permit the use of several positions of the plate holder relative to the target, since no one position of the plate holder probe was suitable for the entire angular scattering range. Position 1 was used for laboratory angles 45° to 55°, position 2 for 55° to 75°, and position 3 for 75° to 87.5°. The projection of the helical path of a typically scattered proton is also shown.

* This work has been supported by the joint program of the ONR and AEC.

† This work is part of a dissertation submitted to the Graduate School of the University of Rochester in partial fulfillment of the requirements for the degree of Doctor of Philosophy.

‡ Present address: E. I. du Pont de Nemours and Company, Argonne National Laboratory, Chicago, Illinois.

[1] C. L. Oxley and R. D. Schamberger, Phys. Rev. **85**, 416 (1952).

[2] In the remainder of this paper all c.m. scattering angles will be designated by the more commonly used supplementary scattering angle of the conjugate proton, although all measurements were actually done with the lower energy backward scattered particle.

[3] O. A. Towler, Jr., Phys. Rev. **84**, 1262 (1951). Also O. A. Towler, Jr., and C. L. Oxley, Phys. Rev. **78**, 326 (1950); Oxley, Schamberger, and Towler, Phys. Rev. **82**, 295 (1951).

[4] Aamodt, Petersen, and Phillips, University of California Radiation Laboratory Report-526 (1949).

B. Target Holder and Targets

The target holder was made in the form of a "*C*" from a thin piece of aluminum rod. All dimensions of the "*C*" were made as large as posssible to reduce scattering from the target holder to a negligible amount. The ends of the target holder were turned to reduce the effective thickness of the target for the low energy scattered protons.

The polyethylene targets were cut in narrow strips 0.32 by 7.3 cm from commercially available polyethylene film. The surface densities ranged from 7.1 to 0.71 mg/cm^2.

For measurements involving high energy scattered protons, the carbon targets used were milled to 17 mg/cm^2 from nearly pure graphite (less than 0.5 percent residue). For scattered proton energies of 15 to 30 Mev, 6 mg/cm^2 carbon targets were employed. These uniform films were prepared by drying a water solution of colloidal graphite (Aquadag). Targets thus prepared had a residue of about 1 percent and a hydrogen content less than 1 percent.

For the very large angle scattering, where the energy of the scattered proton was 10 Mev or less, thin polystyrene $(CH)_n$ targets, 0.3 mg/cm^2, were used for comparison with the polyethylene. These were made by dissolving polystyrene in benzene and floating the film out on water.

C. Plate Holder and Plates

The plate holder was made from solid cylindrical aluminum stock, a quarter section of which had been cut out to provide a flat base for six 1-in. by 3-in. photographic plates. The plates were exposed horizontally with the emulsion side up. Spring clamps held one long edge of the plates to a machined edge of the plate holder and left fiducial marks on the emulsion which enabled accurate determination of the distance of the plate from some known point. The side of the plate which fitted to the machined edge was later the same side which determined the alignment of the plate on the microscope stage. The light shield fitting over the plate holder was provided with a 1.16 mg/cm^2 aluminum window.

The photographic plates were Eastman NTB-3, NTB, or NTA, depending on the energy of the scattered proton. These were developed by standard procedure, maintaining the emulsions horizontal to reduce deformation.

D. Shielding

During an exposure large numbers of nuclear particles, mostly protons, were traveling in the vicinity of the plates near the floor of the tank. The main shielding (Fig. 1) was placed along the axis of the plate holder to prevent protons traveling in the general direction of the beam from striking the plates. This shielding was elevated to prevent protons scattered in the target from

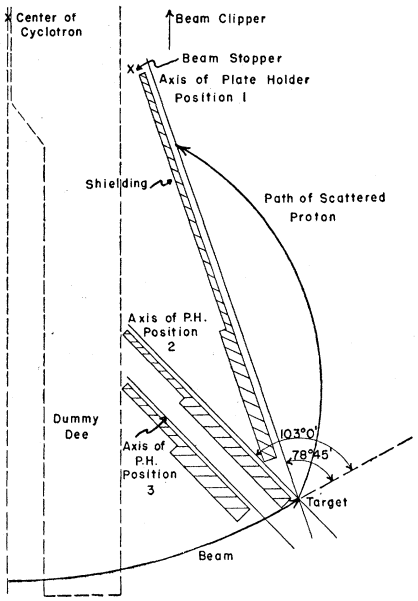

FIG. 1. Arrangement in cyclotron tank.

making more than half a revolution before entering the plates.

A *C*-shaped beam clipper with a 1-inch aperture, introduced in the median plane with the jaws extending to the 59.25-in. radius, was used to reduce the beam height and decrease the number of traversals through the target.

In some of the exposures it was expedient to insert thin vertical strips of copper in the plate holder itself to shadow portions of the plates from low energy protons coming from spurious sources. The direction of these tracks was such as to make them a nonconfusable background, but their deletion made the scanning easier.

An electromagnetically actuated beam stopper was placed at the 13-in. radius to prevent exposure of the plates while the operation of the cyclotron was stabilized.

III. CALCULATION OF SCATTERING ANGLE AND SOLID ANGLE

The determination of the scattering angle can proceed in one of several different ways. The method used was chosen because it was most direct. The general procedure was to measure the mean entrance angle λ_P for proton-proton scattering in a plate at a given distance x, measured in the horizontal plane, from the target. Knowing the vertical separation of the plates and the beam center and the plate holder position, the horizontal and vertical components of the scattering angle θ can be obtained. The radius of curvature of the scattered proton can then be calculated from (1) the scattering angle, the incident proton energy, the energy-scattering angle relationship for p-p collisions, and the magnetic field constants, or (2) geometrical considerations involving λ_P, x, the vertical separation, and the plate holder position. These two independent calcula-

tions of the radius of curvature provide a check on the internal consistency of the calculations and measurements of probe and target positions.

The solid angle was calculated, taking into account relativistic corrections and the effect of the magnetic field on the trajectories of the scattered protons. The solid angle $\Delta\Omega$ subtended at the target by a small area $\Delta a \Delta b$ in the horizontal plane of the emulsion is given by

$$\Delta\Omega = \cos\beta \Delta\beta \Delta\gamma = \cos\beta J\left(\frac{\beta, \gamma}{a, b}\right)\Delta a \Delta b,$$

where β and γ are, respectively, the vertical and horizontal components of the scattering angle θ. The calculation of the Jacobian is rather involved and will not be given here.

The focusing action of the magnetic field tending to return ions scattered from the median plane is negligible in this case, as is the effect on the scattered proton trajectories of the slight increase of the magnetic field from the target to the plate position.

Ideally, the protons scattered by protons in the hydrocarbon target should enter a given position on a plate at only one angle, λ_P. However, a large number of factors tend to spread out the entrance angle. These are the energy spread in the incident beam, the vertical spread of the beam on the target, the energy spread of the scattered protons due to absorption in the target, the angular divergencies in the beam caused by radial and vertical oscillations, the dimensions of the area scanned on the plate, the observer's error in measuring the track angle, and multiple scattering in the target, aluminum window, and emulsion. These effects were estimated and calculated for various scattering angles. The observed entrance angle spread is accounted for largely by factors other than the incident beam energy spread. There is some indication, however, that the energy spread is of the order of 20-Mev full width.

The energy loss per traversal in the targets was small (3 to 10 kev), and it was thought that such particles would be removed by the clipper before the energy loss became considerable. This was borne out by the fact that the entrance angle distributions in the proton-proton peak were not skewed in a manner that would show a rather large lower energy component in the incident beam. Also, the calculated entrance angle agreed very well with the mean of the observed. The fraction of protons striking the target a distance 1.1 in. removed from the median plane, and hence the fraction making large vertical oscillations, was measured by observing the activity in the ends of the strip targets which had been exposed vertically. This fraction varied between 0.01 and 0.03 from run to run. This effect, as well as the radial oscillations, decreases the angular resolution of this method.

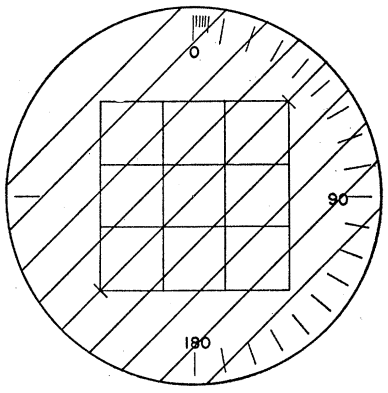

FIG. 2. Protractor eyepiece reticules.

IV. MEASUREMENT OF THE C^{11} ACTIVITY

The C^{11} activity was measured with the calibrated beta-counter described by Oxley and Schamberger.[1] A pertinent point to be stressed is that one of the calibrating sources of the counter had been used by Aamodt, Petersen, and Phillips[4] as a secondary standard in their measurement of the C^{11} production cross section.

V. PHOTOGRAPHIC METHOD

A. Scanning Procedure

The protons which are scattered by protons in the hydrocarbon target enter the plate at certain definite angles which are determined by the energy-scattering angle relation for proton-proton scattering. The protons scattered by the carbon nuclei have no such energy-angle relationship; therefore these carbon scattered protons enter the plate with an angular spread of five to ten times the spread observed for the proton-proton collisions. The scanning problem then is to obtain an angular distribution at a given point on a plate for those protons scattered by a hydrocarbon target, and another angular distribution at the same point on a plate for those scattered by a carbon target. From an exposure to a hydrocarbon target, one would expect to see:

(1) A small number of protons entering the plate at angles far removed from the entrance angle λ_P expected for p-p collisions. These presumably come from other scatterings in the cyclotron tank. (2) A larger number of protons, scattered by the carbon, entering at angles around λ_P. (3) A large number of protons entering at λ_P, which are the protons from the p-p collisions in the target. From a carbon target, one expects only the effects (1) and (2).

Almost all of the scanning was done using a 43× fluorite oil immersion objective and 15× eyepieces. The right eyepiece of the microscope was fitted with a special protractor device by which the angles of the tracks were measured. In the focal plane of the eyepiece lenses were two reticules, one fixed and the other rotatable (Fig. 2).

Etched on the fixed reticule were a square, divided into nine smaller squares, and degree marks, going from

0° to 180°, each degree divided into 20 minutes of arc. The area of the large square, which defined the solid angle, was calibrated with a Bausch and Lomb micrometer disk. The division into nine smaller squares facilitated the counting. On the rotatable reticule were etched a group of parallel lines, the center line of which was diametric and distinguished by two small intersecting lines. This center line read the entrance angle when a proton track was aligned with one of the parallel lines.

We will now consider the criteria used in the selection of tracks. A track, to be counted, must begin in the surface of the emulsion and within the area described by the large square. A track must have a dip angle that is close to the calculated one to be counted. Tracks which dived steeply or just skimmed the surface of the emulsion were not counted, because these could not have come directly from the target. There were a few very heavy thick tracks which were obviously (from the delta-ray density) particles with $Z \geq 2$. These were not counted, as well as some low energy proton tracks which ended in the emulsion. An exception to this last rule occurred when observations were made on scattered protons expected to end in the emulsion. All other tracks were counted.

When it was decided that a track was to be counted, and if the track entered at an angle plus or minus 5° from λ_P, the microscope field was moved slightly to place the track directly beneath one of the parallel lines. Then the angle was recorded and the field moved back to its original setting. This was done by taking certain grains or tracks intersecting the lines of the squares as fiducial marks and not by the verniers on the stage. Tracks which entered at angles beyond the plus or minus 5° mentioned above were not lined up by moving the field, but by setting the closest parallel line parallel to the track. An experienced observer could do this within 20 minutes of the real angle of entrance of the track. To reduce the labor involved, only certain ranges of entrance angle were measured for each area.

Three observers collected the final data. Frequent spot checks were made between the author and the other two observers. Since it was impractical to rematch all the fields scanned by one observer, areas within the same coordinates were scanned by different observers to determine any differences in the method of counting or measuring the tracks. In these checks, the number of tracks per degree of entrance angle counted by each observer agreed to within 3 percent, which was better than allowed by the statistical fluctuations.

B. Determination of the Number of Scattered Protons

When the entrance angle distribution is obtained for the protons scattered by a hydrocarbon target, the effect due to the proton-proton collisions is quite obvious, as is the effect due to carbon collisions. One may make a fair estimate in determining the number of proton-scattered protons by counting those in the peak above a smooth curve drawn to fit the distribution for carbon scattering outside the peak. However, the actual shape under the p-p peak of the proton distribution from carbon collisions is of some importance, and therefore proton distributions were obtained from carbon targets. They were matched to the hydrocarbon distributions by correcting for the incident beam in the two exposures. The actual number of protons scattered by protons was obtained by subtracting the number of tracks given by the carbon data under the peak, using a smoothed curve, from the actual number of tracks in the peak of the hydrocarbon data.

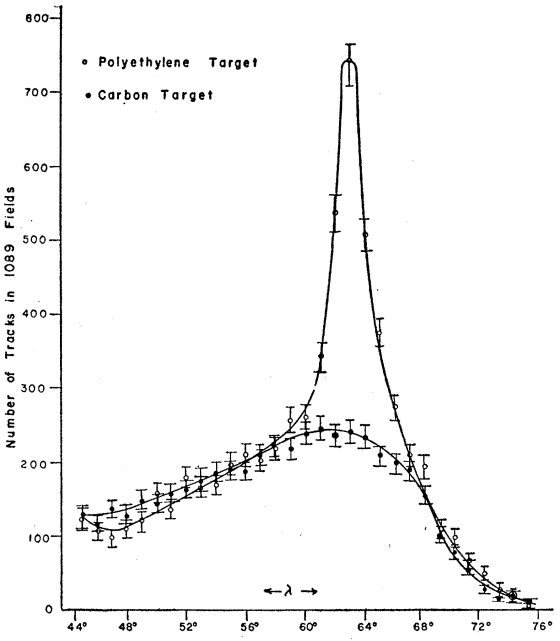

FIG. 3. Entrance angle distribution for $\theta = 52.4°$.

The proton distributions from the carbon collisions in the two targets matched very well in absolute value and shape for all angles except one ($\theta = 70.6°$), and in this one case an additional factor had to be applied to the carbon target distribution in order to match the absolute value of the distribution for the hydrocarbon target. This is perhaps justified by the fact that spurious sources and beam distribution may change over a short period of time, which might affect the actual number scattered into this one plate. Other plates exposed in the same runs as the one in which the discrepancy occurred produced good agreement between the polyethylene and carbon data, and it is difficult to see that the number of protons in the proton-proton peak could be affected except by a small amount due to the shape of the corrected carbon distribution under the peak.

The distributions obtained for the scattering angles 52.4°, 83.1° and 85.4° are shown in Figs. 3, 4, and 5. The distributions for the other five scattering angles observed are similar to that shown in Fig. 3.

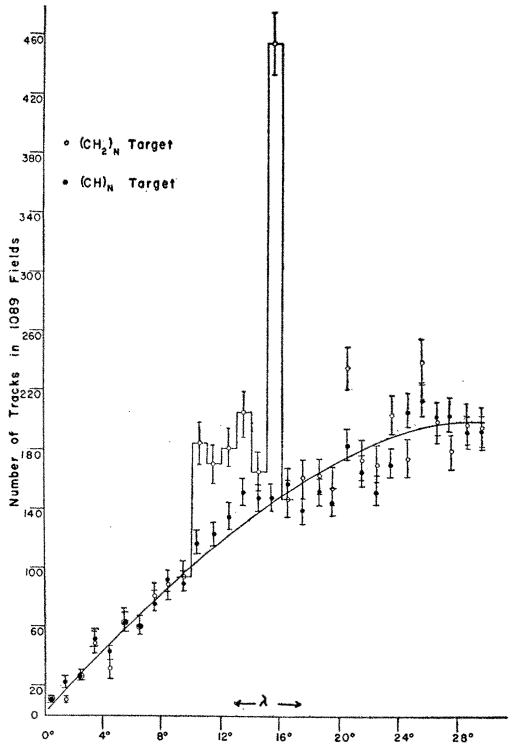

FIG. 4. Entrance angle distribution for $\theta=83.1°$.

For the two large scattering angles, 83.1° and 85.4°, data were taken for polyethylene $(CH_2)_n$ and polystyrene $(CH)_n$ targets. Any pure carbon target that could be made, inserted, and removed from the tank was still too thick for the energies of the protons involved. The polystyrene distribution was taken mainly to check the shape of the proton spectrum from carbon on sides adjacent to the proton-proton peak. In these two cases, a smooth curve was drawn through the sides adjacent to the peak and this curve was used for subtraction purposes. A cross section could be obtained from the polystyrene data alone, using the same subtraction process, but the statistical errors are very large. (However, the cross sections obtained from the two types of hydrocarbon targets agreed within the errors.)

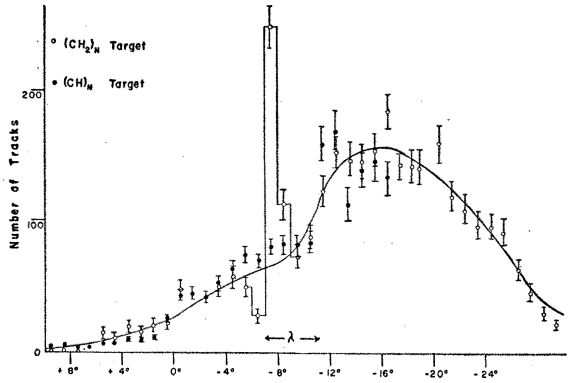

FIG. 5. Entrance angle distribution for $\theta=85.4°$.

TABLE I. Number of proton scattered protons for each scattering angle.

θ	N_{CH_2}	N_C	N_P	Mean error (%)
52.4°	3682	2174	1508	5.07
66.1°	1133	384	749	5.27
70.6°	992	343[a]	649	5.64
75.0°	3435	1888	1547	4.72
75.6°	647	293	354	8.67
80.1°	2492	1560	932	6.83
83.1°	1359	750[b]	609	7.50
85.4°	360	135[b]	225	9.90

N_{CH_2}=number of protons from polyethylene.
N_C=number of protons from carbon.
[a] Number of tracks corrected by 38 percent to match sides of CH_2 peak.
[b] N_C taken from smooth curves drawn through base of peak, based on CH_2 and CH data.

The number of proton-scattered protons, N_P, is shown in Table I. The error assigned to N_P is the mean statistical error considering the background subtraction.

Data for the scattering angles 70.6° and 75.0° were obtained from the same exposure and probe position for both the polyethylene and carbon target. The polyethylene data for the angles 75.6°, 80.1°, 83.1°, and 85.4° were obtained from the same exposure and probe position, as were the carbon data for the first two of these angles and the polystyrene data for the last two. The first two scattering angles in Table I were measured with probe position 1, the second two angles with probe position 2, and all the others with position 3. A check of the consistency of the cross sections obtained in different runs at different probe positions is provided by the agreement of the cross sections at laboratory angles 75.0° and 75.6°.

VI. DIFFERENTIAL CROSS SECTION

The experimental results and the cross sections are given in Table II, and the cross section in the center-of-mass system is plotted in Fig. 6.

The errors assigned to the cross section are the relative mean errors in the determination of N_P. These errors are valid for the relative values of the cross sec-

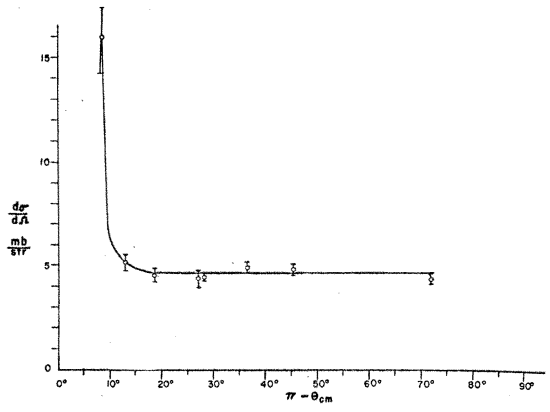

FIG. 6. Differential scattering cross section at 240 Mev. The assigned errors are the statistical errors only.

TABLE II. Experimental results.

$\pi-\theta_{c.m.}$	$\theta_{c.m.}$	θ	N_P	N_C	$\Delta\Omega$	Lab cross section mb/sterad	$\frac{\Delta\Omega}{\Delta\Omega_{c.m.}}$	c.m. cross section mb/sterad	Resolution (c.m.)
71.9°	108.1°	52.4°	1508	9.033×10^{8}	4.002×10^{-6}	10.22	0.4241	4.33±0.22	1.6°
45.2°	134.8°	66.1°	749	5.852	4.376	7.165	0.6713	4.81±0.25	1.3°
36.6°	143.4°	70.6°	649	2.931	9.187	5.905	0.8293	4.90±0.28	1.3°
28.3°	151.7°	75.0°	1547	2.931	31.33	4.129	1.072	4.43±0.21	1.2°
27.2°	152.8°	75.6°	354	2.413	9.183	3.837	1.119	4.38±0.38	1.2°
18.6°	161.4°	80.1°	932	2.413	33.72	2.807	1.636	4.59±0.31	1.5°
13.0°	167.0°	83.1°	609	2.413	28.01	2.207	2.336	5.16±0.39	2.1°
8.7°	171.3°	85.4°	225	2.413	5.038	4.535	3.482	15.8±1.6	2.4°

tions in this experiment. The absolute value of the cross section depends upon the calibration of the beta-counter, the $C^{12}(p,pn)C^{11}$ cross section, calibration of the microscope field areas, relative position of the target and plate holder probes, the incident energy and perhaps unknown systematic errors. The error in the calibration of the beta-counter is 4 percent, and in the $C^{12}(p,pn)C^{11}$ cross section 6 percent. The error due to the other factors mentioned above is estimated to be 6 percent, giving a total error in the absolute value of the cross section of 9 percent.

The experimental cross section exhibits the previously observed flat behavior down to a c.m. angle of about 15°, and then increases by a factor 3.5 over the isotropic average at 8.7°. The laboratory cross section increases by a factor two in going from a scattering angle of 83° to 85°. The sharp increase at 8.7° is certainly due to Coulomb effects, while the extreme flatness in the region preceding this is probably due to interference terms.

The averaged value of the observed cross section in the center-of-mass system (excluding the value for 8.7°) is 4.66±0.39 mb. This assigned error includes the absolute errors mentioned above and a 2.3 percent statistical error, based on the observation of 21,132 tracks for the seven angles.

The angular resolution of this method depends upon the area of the plate scanned, the energy spread of the incident beam, the vertical spread of the beam on the target, the energy loss in the target, the angular divergence of the beam, and the multiple scattering of the recoil proton in the target. The resolution for each of the eight angles measured is given in Table II.

VII. COMPARISON OF RESULTS

The agreement between this experiment and that of Oxley and Schamberger[1] at the same energy is good. Their average value of the cross section, measured from 27.5° to 90°, is 4.97±0.43 mb/sterad. When the mutual errors in the $C^{12}(p,pn)C^{11}$ cross section and the calibration of the beta-counter are subtracted, the relative error in both of these experiments is 0.22 mb. The combined value for the isotropic portion of the cross section obtained by these two experiments is 4.81±0.38 mb/sterad.

These results are higher by about 30 percent than the value of 3.6±0.2 mb/sterad obtained by Chamberlain, Segrè, and Wiegand.[5] We have done some work at this laboratory in determining the *p-p* scattering cross section using carbon detectors throughout and referring only to the slope of the C^{11} production cross section curve. Preliminary results favor the higher values of the cross section.

VIII. ACKNOWLEDGMENTS

I wish to thank Professor C. L. Oxley, who originally suggested this method of attacking the problem, for many helpful suggestions during the course of this work. I also wish to express appreciation to Miss Evelyn Kohn for her work at the microscope, and to the cyclotron crew under the direction of Mr. Hugo Logemann.

[5] Chamberlain, Segrè, and Wiegand, Phys. Rev. **83**, 923 (1951).